IEEE Access
Multidisciplinary | Rapid Review | Open Access Journal

Received 14 October 2023, accepted 28 October 2023, date of publication 1 November 2023, date of current version 7 November 2023.

Digital Object Identifier 10.1109/ACCESS.2023.3329067

RESEARCH ARTICLE

Three-Dimensional Information Modeling Based on Incomplete Data for Anchor Engineering

ZHANG SONGAN, HU WEI, ZENG LIANG, YANG JUNJIE, ZHONG YUSEN, LIU ZHEN, AND ZHOU CUIYING

School of Civil Engineering, Sun Yat-sen University, Zhuhai 519082, China
Guangdong Engineering Research Centre for Major Infrastructure Safety, Sun Yat-sen University, Guangzhou 510275, China
Research Center for Geotechnical Engineering and Information Technology, Sun Yat-sen University, Guangzhou 510275, China

Corresponding authors: Liu Zhen (liuzh8@mail.sysu.edu.cn) and Zhou Cuiying (zhoucy@mail.sysu.edu.cn)

This work was supported by the National Natural Science Foundation of China under Grant 42293354, Grant 42293351, Grant 42293355, Grant 42277131, and Grant 41977230.

ABSTRACT Intelligent design is a trend in geotechnical engineering. However, a middle link between demand identification and intelligent design is missing in anchor engineering, resulting in lower efficiency in terms of the interaction between the anchor components, geological body and modeling information. To address this challenge, this paper proposes a method for modeling a three-dimensional anchor engineering information model based on sparse boreholes. This method includes three parts: modeling the geological body, integrated modeling of the anchor components and the geological body, and multiple information assignments based on the anchor model. The feasibility was validated in actual engineering scenarios by using neural networks and rendering engines. The results showed that the prediction accuracy of the strata improved by 17.69%, the modeling efficiency increased by double, and engineering information was fit to the model well. This paper has the application potential to achieve intelligent design in anchor engineering.

INDEX TERMS Artificial neural networks, building information management, digital simulation, geoengineering, information processing, land surface, machine learning, numerical models, space mapping, solid modeling.

I. INTRODUCTION

Anchor engineering involves structural engineering that is focused on securing or reinforcing rock and soil bodies and is widely used in pits, bridges, slopes and other projects. In the intelligent design of anchor engineering, a three-dimensional (3D) information model plays a crucial role. Information model technology aims to digitally represent and simulate three-dimensional characteristics, including the structure of anchor engineering, the distribution of anchor components, and the geological conditions of a construction site [1], [2]. Through a three-dimensional model, designers can gain a more intuitive understanding of the structural composition and spatial layout of anchor engineering, facilitating effective problem identification, solution generation, and calculation of various project indicators [3], [4].

The associate editor coordinating the review of this manuscript and approving it for publication was Gerard-Andre Capolino.

A. MODELING METHODS AND TOOLS

An information model in anchor engineering mainly includes the geological body and anchor components.

In terms of modeling data, methods include field surveys, borehole exploration [5], geophysical investigations [6], satellite remote sensing [7], unmanned aerial vehicle platforms [8] and in situ tests [9]. Among these methods, geophysical methods are appropriate for gathering intricate terrain data due to their advanced technology and precise results. In comparison, boreholes are widely used in engineering owing to their mature technology, broad applicability, and cost-effectiveness. Numerous experimental studies have been conducted to obtain mechanical performance data for different anchor materials, lengths, diameters, and anchoring methods [10], [11]. These experimental data, including the prestress level, bearing capacity, deformation characteristics, and fatigue performance of the anchor, serve as a fundamental basis for designs and models.

In terms of modeling methods, various interdisciplinary approaches have been proposed. Due to the spatial variability of the stratigraphy, geotechnical parameters usually lack completeness and need to be reconstructed. A feasible way to fill information gaps is through geophysical methods, such as those used by Matteo Rossi [12], who implemented distributed acoustic sensing to reconstruct the geotechnical parameters. Geostatistical analysis methods [13], [14], such as the inverse distance weighting and kriging methods, have been widely used in stratum interpolation for model construction. Jia, QR [15] improved the kriging method, which can be applied to generate a faulted geological surface. Topological information from stratum modeling is another common modeling method that can be used to build a solid model. Zeng, Qinghe proposed a three-dimensional stratum model based on topological solid structure [16]. In addition, the Bessel spline and hybrid surface methods were used for constructing a complex model [17].

In terms of modeling tools, many software programs are available for constructing anchor engineering models, such as ''AutoCAD'', ''Revit'', and ''Google SketchUp'' [18], [19], [20]. These tools assist engineers in creating accurate three-dimensional information models. Some geographic and survey techniques have also been used for geological modeling. Laser scanning technology is a valuable tool used in elaborate modeling, allowing engineers to rapidly capture field data and build precise three-dimensional models [21]. This technology is commonly employed in extensive projects such as bridges and landslide anchor engineering. Geoinformation technology, such as geographic information systems (GISs) and digital geological maps, has also been utilized to construct complex three-dimensional information models [22].In practical applications, the careful consideration of various factors and appropriate selection of modeling methods and tools are essential, especially in the presence of complex geological bodies, diverse anchor component shapes, and incomplete data.

B. CHALLENGES AND WORKS

Most of the modeling methods mentioned above require large amounts of data of various types. In most engineering applications, the data that reflect the geological conditions of the site are mainly derived from the borehole, which serves as the primary source for modeling. The primary type used is the stratum borehole. Others are only a few hydrological and geothermal boreholes. Therefore, building a three-dimensional information model for anchor engineering encounters challenges related to incomplete data. Geostatistical methods can contribute to addressing the issues with missing stratum data. For example, Xiulan He [23] proposed a multiple-point statistical method that can simulate the geological conditions of buried valleys well by combining existing geological models and detailed geophysical data, especially for limited boreholes. A neural network algorithm plays a vital role in feature selection and data analysis when large amounts of data are available. Junhong Zhao explored the relationship between geological types and drilling data and accurately predicted the geological types of strata [24]. Both of these methods can be used to optimize the modeling process in the presence of necessary boreholes.

In addition, the relation between general design requirements and specific component parameters is not well-established. The parametric information model can address this problem and plays an essential role in intellectual design [25]. Numerical models containing mechanical data, geological data, vector and raster data can be used not only for visualization but also for design checking. Several methods have been explored to assign engineering information to three-dimensional models [26], [27], including the grid model, point cloud model, vector model, etc.

C. CONTRIBUTIONS AND INNOVATIONS

To help designers in anchor engineering, this paper proposes a three-dimensional modeling method of an information model based on incomplete data. This method is based on a neural network algorithm that improves the training process, increases the model accuracy and elaborates the modeling principle with a foundation slope engineering example. The focus of this method is to enable the reconstruction of sparse data by making connections between surrounding boreholes. Moreover, the design of anchor components by stratigraphic model parameters is achieved. In addition, the intellectual design of anchor engineering requires digital engineering information. However, demand, limitation and other data are currently nonnumerical. Thus, these data cannot provide specific references for subsequent anchor component design and modeling. In this paper, three-dimensional visualization techniques and interpolation are used to implement the information to model assignment process.

The proposed method is more universal and practical because it uses drill results as a source of modeling data. The problem of low modeling efficiency and accuracy due to sparse data in anchor engineering is solved. After the modeling is completed, the transition from demand identification to intelligent design is achieved by mapping the engineering information numerically to the model. The results show the potential of this method to be generalized for intelligent design in anchoring engineering.

II. RESEARCH CONTENT AND METHODOLOGY

A. PRINCIPLES FOR INCOMPLETE DATA MODELING FOR ANCHOR ENGINEERING

Incomplete data in anchor engineering refers to the presence of missing, erroneous, or noisy datasets that fail to fully represent the characteristics and properties of anchor engineering systems [28]. When constructing three-dimensional models of anchor engineering, incomplete data are a common challenge. Data for anchor engineering modeling are typically gathered from sources such as geological exploration reports and anchor component parameter

reports. For various reasons, certain data may be missing or contain errors. Incomplete data modeling methods aim to enhance the quality and utility of the data by addressing missing, erroneous, and outlier data points. These methods involve data processing techniques such as data cleaning, prediction, and interpolation, which contribute to improving the reliability of the data and reducing errors in data analysis and modeling. The approach of incomplete data modeling is not limited to anchor engineering alone; it can also be applied in various other engineering fields, including tunnel construction, geotechnical engineering, computer science, and other fields [29]. Establishing an incomplete data modeling system enables the generation of more comprehensive, accurate, and reliable data for analysis and modeling, thereby enhancing the support provided for engineering decision-making and management.

Incomplete data modeling in anchor engineering mainly includes incomplete data modeling of the geological body and incomplete data modeling of anchor components, as shown in Fig. 1. Three-dimensional modeling of incomplete geological data is a complex problem that requires the consideration of various techniques and tools and accounting for the data characteristics, modeling objectives, and suitability of chosen methods and tools. The processing of incomplete data is based on the features of the borehole and the technique of geological modeling:

(1) The original data for three-dimensional modeling of the geological body are sourced from the borehole data. However, there may be a small number of boreholes with a uneven distribution, leading to incomplete data issues such as missing or incorrect data in certain areas. To address this, the dataset is reconstructed through operations such as subdividing strata and using nearby boreholes as central borehole input variables. The reconstructed dataset is then utilized for training a back propagation (BP) neural network [30] to select the optimal model for prediction and interpolation, resulting in three-dimensional data and geological body models that can be visualized. Other neural networks can also be used in strata prediction.

(2) For anchor components, the primary data source is the anchor design scheme, which provides parameters such as length, angle, and spacing. However, these parameters alone are insufficient for three-dimensional modeling of the anchor components and do not constitute complete datasets.

To overcome this, the anchor parameters are processed by considering the construction characteristics of the anchor and referencing the coordinate system of the three-dimensional geological body model. By determining the coordinates of the starting position of the anchor drilling and the geological body boundary coordinates, the coordinates of each borehole in the reference system of the geological body model and the anchor data model are obtained. This process enables the generation of a three-dimensional anchor model by visualizing the data model. By addressing the incomplete data modeling of both the geological body and anchor components, a more comprehensive and accurate three-dimensional model of anchor engineering can be achieved.

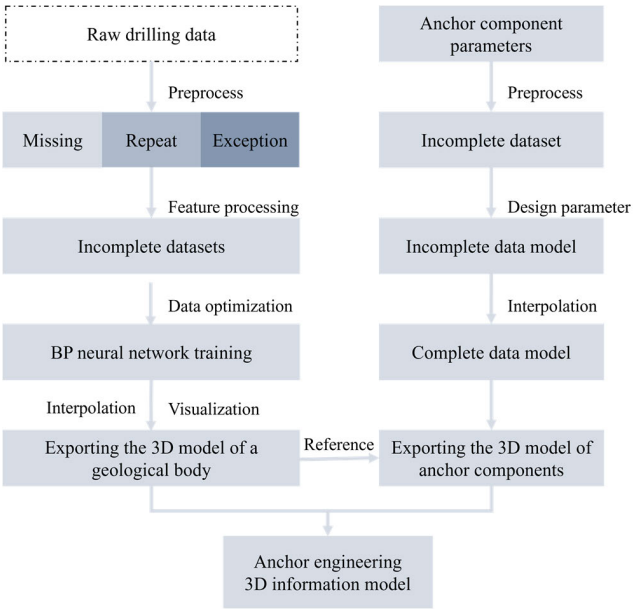

FIGURE 1. Modeling workflow of anchor engineering based on borehole data. The left part is the modeling process of the geological body, and the left part is the modeling process of the anchor components.

B. INCOMPLETE THREE-DIMENSIONAL GEOLOGICAL BODY MODELING BASED ON THE SUBDIVIDED STRATUM FEATURE

1) THREE-DIMENSIONAL GEOLOGICAL BODY MODELING

The main steps in three-dimensional geological body modeling using machine learning algorithm include processing of data feature engineering, training machine learning algorithms based on geological body modeling, cross-validation of training models in groups, and visualizing geological body data models. The feature engineering [31] necessary for three-dimensional geological modeling of anchor engineering involves transforming raw borehole stratum data into a input variable–output variable format consisting of descriptive features. This format enables the training model to attain optimal results.

The primary data source for modeling the geological body is geological survey reports, which include geological information such as the borehole log. The borehole log provides stratigraphy data, including the location coordinates, stratum categories and parameters, and stratum thickness. To meet the requirements of machine learning algorithms, which typically require data in a standard value format, the data extracted from a borehole histogram need to be structured accordingly. This structuring process involves extracting features such as the hole number, X- and Y-coordinates, stratum category, hole elevation, and layer thickness for each stratum. Through this structuring process,

the data can be used to build effective and generalizable training and testing models for machine learning algorithms.

The $Z-$direction coordinates of the stratum are calculated using the central elevation of each stratum to obtain a more accurate model, as shown in (1):

$$Z_i = H - \sum_{i=0}^{i-1} h_i - \frac{h_i}{2} \tag{1}$$

where Z_i is the elevation of the strata i (center of strata), H is the elevation of the borehole, and h_i denotes the thickness of the stratum i at the borehole location. The coordinates and stratum thickness are used as input variables, while the stratum type serves as the output variable. Since the evaluation indicators have different scales and units, data normalization is necessary to ensure consistency. Data normalization involves scaling the data within a certain range to facilitate algorithm training. Each row of data (location coordinates, stratum thickness, and stratum type) is normalized using the formula shown in (2).

$$\mathrm{y} = \frac{(y_{max} - y_{min}) \times (x - x_{min})}{x_{max} - x_{min}} + y_{min} \tag{2}$$

Here, y, y_{max} and y_{min} are the results of data normalization, the maximum value of the processing data, and the minimum value of the processing data, respectively, and x_{max} and x_{min} are normalized range parameters, typically $[-1,1]$ and [0, 1], respectively. Following the feature processing of the borehole data, the data are trained using a three-layer BP neural network. This neural network is a nonlinear algorithm consisting of an input layer, an output layer, and a hidden layer. The input layer contains nodes corresponding to the features, such as the stratum position coordinates and layer thickness. The output layer contains nodes representing the target values, which in this case are the stratum types. The optimal number of nodes in the hidden layer is typically determined through experimentation and trial-and-error.

Through continuous iterative training, the BP neural network aims to optimize the curve fitting of the borehole stratum data, thereby enhancing the model's accuracy, as shown in Fig. 2. Notably, simulating homogeneous and regular stratum data curves is relatively easier compared with discrete and disordered ones, which pose greater challenges and yield lower fit results.

Once the geological body data model is obtained, it can be visualized using the Three.js browser rendering engine, which is based on the WebGL three-dimensional drawing protocol [32]. The workflow of the above modeling methods is shown in Fig. 3.

2) OPTIMIZATION OF MACHINE LEARNING CONSIDERING ACTUAL ENGINEERING CHARACTERISTICS

The number of exploration boreholes typically falls short of the data requirements for machine learning algorithms, although it is sufficient for engineering design purposes. The scarcity of learning data poses a common and challenging issue in the process of geological modeling and hinders the use of neural network algorithms.

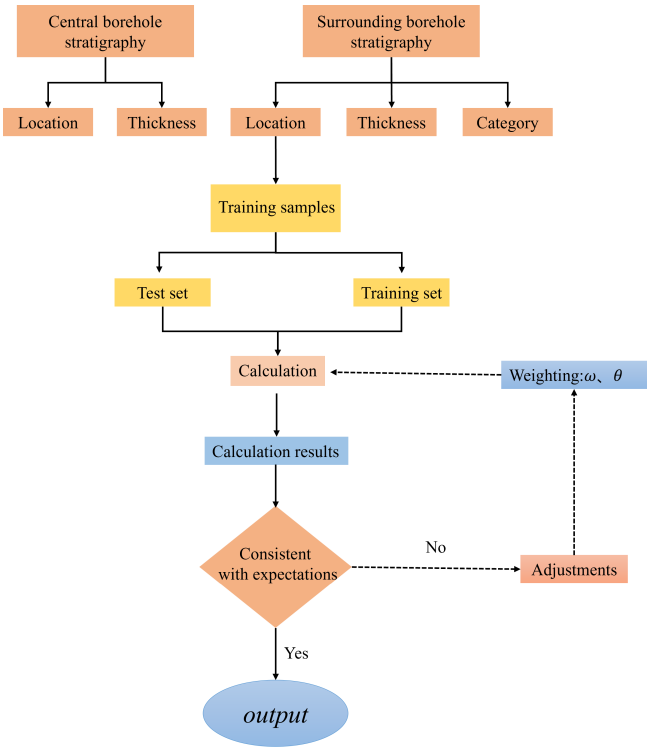

FIGURE 2. Workflow of stratigraphy prediction by a back propagation neural network. The training sample should be processed according to (2) before input.

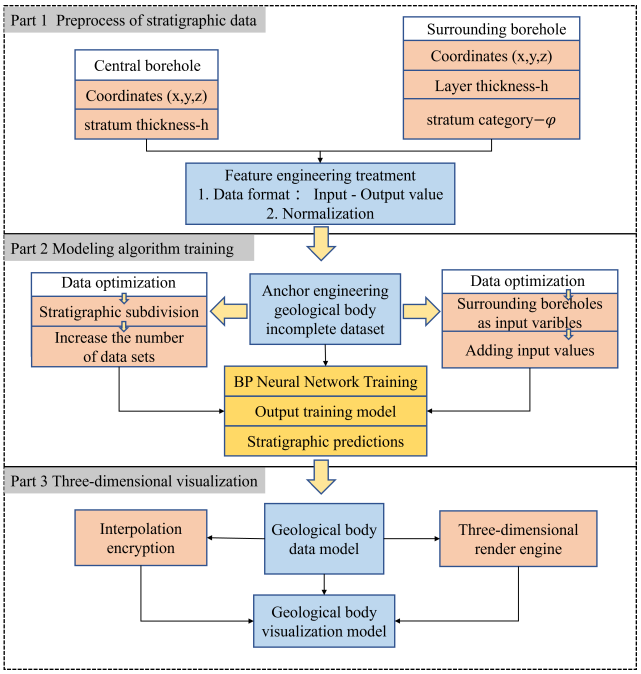

FIGURE 3. Modeling and visualization workflow of the geological body. The first part involves extracting the stratigraphy data from the borehole log, the second part includes predicting the stratum by neural network algorithms, and the third part involves visualizing the predicted model.

To address these problems, the original data are reprocessed by considering engineering characteristics. The bore-

hole data consist of multiple strata, each with a thickness of 1 m-12 m. Due to the large thickness of these layers, the number of layers is too small for use as a sample set for machine learning. Therefore, each stratum is subdivided into N substrata, as shown in Fig. 4. This approach can not only reconstruct the stratum data and increase the amount of stratum data (the BP neural network needs considerable data), but it can also increase the accuracy of stratum prediction.

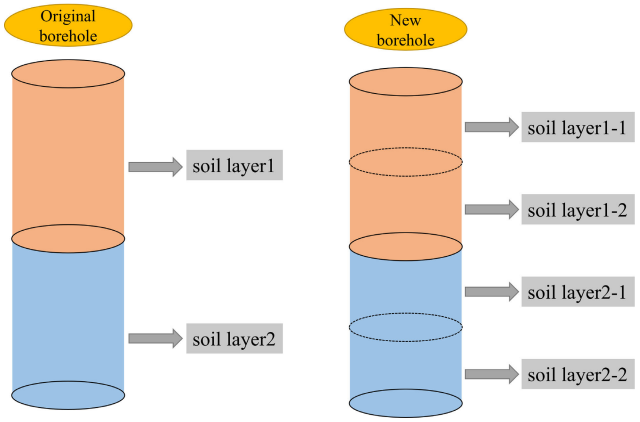

FIGURE 4. Process of subdividing the stratigraphic data obtained from boreholes into multiple sub-stratigraphic layers. The left part is the original stratigraphy dataset from the borehole log, and the right part is the new dataset.

The effectiveness of machine learning training is influenced by factors such as the number of data, the number of features, and the target value. These factors determine the algorithm's upper limit and guide the continuous adjustment of the algorithm and its parameters to approach that limit [33]. While stratum subdivision can increase the data count, the extracted features, namely, the borehole stratum coordinates and layer thickness, are limited. To expand the number of features, the surrounding boreholes' stratum data can be incorporated as additional features for the central borehole stratigraphy, as depicted in Fig. 5. By utilizing these crucial influencing factors, the stratum category can be better determined.

Given the extracted borehole histogram data, Equation (3) illustrates that only the borehole stratum position coordinates and layer thickness serve as features.

$$D = f\ (x, y, z, c) \tag{3}$$

However, the addition of features significantly increases the total count, as demonstrated in (4), thereby further enhancing the effectiveness of the machine learning training.

$$D' = f\ (x, y, z, c) + \sum_{i=1}^{n} f(x_i, y_i, z_i, c_i) \tag{4}$$

Here, x and y are the coordinates of the borehole position, z is the elevation of the center of the borehole stratum, c is the stratum thickness of the borehole, n is the number of surrounding boreholes, and D and D' are the target values for the stratigraphy before and after the data process, respectively.

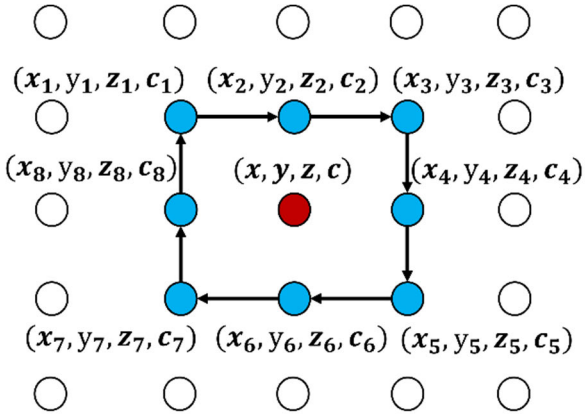

FIGURE 5. Location relationship between the center borehole and the surrounding boreholes. The letters *x*, *y* and *z* are the coordinates of the borehole position, and the letter c is the stratum thickness of the borehole.

C. EFFICIENT FUSION MODELING OF GEOLOGICAL BODY ANCHORS

1) INTEGRATED THREE-DIMENSIONAL MODELING OF ANCHOR COMPONENTS

Anchor components, such as grouted anchors, anchor cables, soil nails, and reinforced soils, are essential for geotechnical reinforcement support [34]. In this paper, threaded metal anchors are used as an example; however, these principles can also be applied to other anchor types. Anchor component parameters include their geometry, position coordinates, length, and angle. To facilitate modeling, these input parameters need to be appropriately processed to align with the requirements of the browser rendering engine. An anchor component typically consists of an anchor body and a base plate, as depicted in Fig. 6.

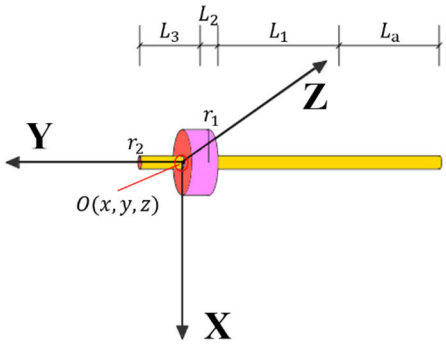

FIGURE 6. Composition and parameters of anchor components. Here, L_1, L_2 and L_3 are the upper length of the anchor body, the length of the base plate, and the lower length of the anchor body, respectively. L_a is the anchorage length.

The information parameters, such as the lengths of the anchor body and base plate, require processing. The center coordinate $O_1(x, y, z)$ is determined by the center of the plate surface on the base plate, while r_1 represents the radius of the base plate, and r_2 represents the anchor body radius.

The Three.js rendering engine is employed to model the anchor member. Equation (5) is used for scoping the base plate, while (6) is employed to model the anchor body. The geometric parameters of the anchor are processed according to the formulas that are implemented as built-in function interfaces. By utilizing these formulas, the data model of the anchor is obtained, integrated with the anchor body, and rendered and visualized using render engine. This completes the three-dimensional modeling of the anchor.

$$\int_{-L_2}^{0} \pi r_1^2 dy \tag{5}$$

$$\int_{-L_1-L_2-L_a}^{L_3} \pi r_2^2 dy \tag{6}$$

2) FUSION MODELING BY INTEGRATING THE GEOLOGICAL BODY AND ANCHOR COMPONENTS

A early method for three-dimensional modeling of anchor components was proposed. This method enables the modeling of anchor components based on their geometric parameters. However, certain parameters, such as the anchorage length, anchorage angle, and anchor component spacing, need to be determined in relation to the geological body. By combining both sets of parameters, the three-dimensional fusion modeling of anchor elements within the geological body can be achieved. Prior to constructing the anchor components, the positioning point for the anchor is determined. This positioning point, denoted as $O(X_1, Y_1, Z_1)$, is located at the boundary of the geological body, as shown in Fig. 7. The position coordinates of the anchor components are determined based on the positioning coordinates and the anchor spacing. By employing (5) and (6), the numerical model of the anchor components is obtained and visualized, facilitating the three-dimensional representation of the anchor components.

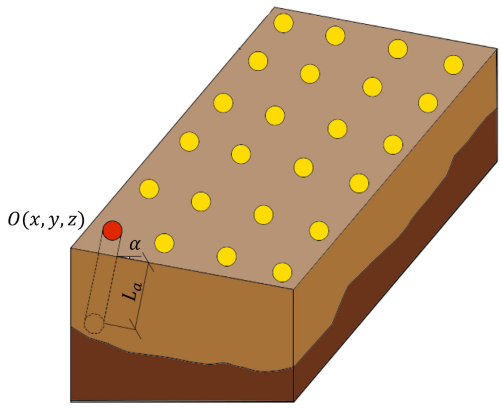

FIGURE 7. Schematic diagram of anchor components embedded in the geologic body. The point *O* is the coordinate of the anchor components' position. L_a is the anchorage length. α is the cross section.

In the fused modeling process, considering grouting as an integral part of anchor construction is crucial, especially when modeling the grouting bond surface, which is helpful for understanding the interaction between the components and the bond. To build a highly reliable three-dimensional model, the modeling process should account for the construction procedure and the relevant structural mechanisms. During the three-dimensional modeling process, geometric parameters such as the thickness of the bonding surface are determined by considering factors such as the size of the anchor borehole and the size of the anchor body. These parameters play a crucial role in accurately representing the characteristics of the grouting bond surface within the model. As shown in Fig. 8, by incorporating these considerations, the three-dimensional model can provide valuable insights into the behavior and performance of the anchor system. The diameter calculation of the anchor component is shown in (7):

$$r = r_1' - r_2' \tag{7}$$

where r, r_1', and r_2' are the bonding surface thickness, the anchor drill hole radius, and the anchor radius, respectively.

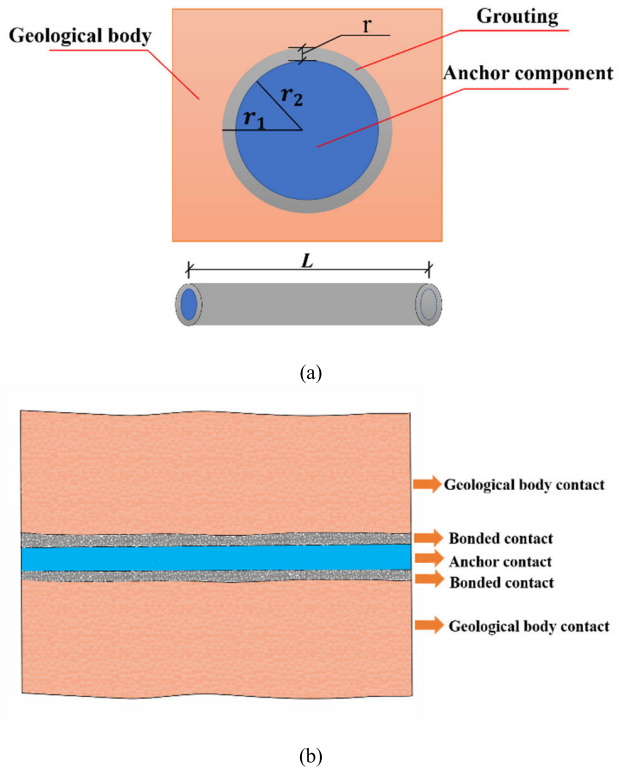

FIGURE 8. Contact surfaces between anchor components and the geological body: (a) is the cross section and illustrates the anchor composition; (b) is the side section and illustrates the interaction.

The depth of the anchor borehole determines the length of the bonding surface. In the modeling process, the length parameter is the depth L of the anchor component, and the length parameter is greater than the anchorage length of the anchor, as shown in (8):

$$L > L_a \tag{8}$$

where L and L_a are the bonding surface length and the anchorage length of the anchor, respectively.

The visualization of the three-dimensional model in anchor engineering relies on the utilization of visualization tools [22]. In visual scenes, the fundamental building blocks are the scene, camera, and renderer [35]. The scene serves as a container that holds various elements, such as lights and models. The scene has a central position with coordinates (0,0,0), and the coordinates of the geological body and anchor components are defined within the scene's right-angle coordinate system. During the modeling process, these two models must be necessarily fused. In considering the construction process of anchor engineering, the anchor components are positioned first, followed by drilling into the stratigraphy. Therefore, the anchor components are prioritized in terms of modeling and fusion within the overall three-dimensional model. By establishing this priority, the resulting visualization accurately represents the interaction between the anchor components and the geological body, providing a comprehensive understanding of the anchor engineering system.

D. MULTIPLE INFORMATION ASSIGNMENT FOR ANCHOR ENGINEERING

Once the three-dimensional model of anchor engineering is established, various pieces of information can be assigned to the model. Specifically, each individual point is assigned real mechanical parameters and monitoring data. To visualize and represent engineering information effectively, the ECharts technology stack, which is capable of rendering the unit points based on their assigned values, is utilized in this paper. This rendering process operates on the principle of a numerical mapping relationship. By inputting a color (r, g, b) into the mapping function, a corresponding new color (R, G, B) is obtained. The specific mapping relationship used for this purpose is shown in (9):

$$(R, G, B) = f\,(r, g, b) \tag{9}$$

Here, (R, G, B) is the superimposed color value.

Based on the (R, G, B) values, the system calculates the maximum and minimum (R, G, B) values before rendering the unit points. Finally, the color corresponding to each color value is obtained, as shown in Fig. 9.

Many discrete points can be obtained, based on the input data. For areas where color values are not mapped, the default ECharts mapping assigns point N_3 the same value as that of the nearest point, which has already been assigned data. In this paper, the ECharts source code is modified to use interpolation, as shown in (10).

$$(R, G, B)_3 = \begin{pmatrix} \delta_i R_i + \delta_{i+1} R_{i+1}, \\ \delta_i G_i + \delta_{i+1} G_{i+1}, \\ \delta_i B_i + \delta_{i+1} B_{i+1} \end{pmatrix} \tag{10}$$

where R_i, G_i, and B_i are the channel color values of the assigned discrete points, and $i = 1$. Here, δ_1 and δ_2 are the weighting factors, as calculated by (11):

$$\delta_i = \frac{h_i}{h}\,(i = 1, 2) \tag{11}$$

where h is the distance between discrete points N_1 and N_2 and h_i is the distance from the assigned discrete point to the unassigned discrete point.

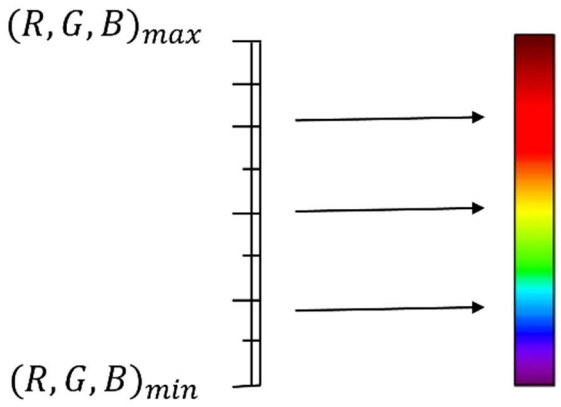

FIGURE 9. Mapping process from the number to the color. $(R,G,B)_{max}$ and $(R,G,B)_{min}$ are the maximum and minimum of the calculated values, respectively.

As shown in Fig. 10, the discrete point N_3 has not been assigned mechanical properties, and N_1 and N_2 are the nearest points to N_3. The color values can be assigned utilizing linear interpolation.

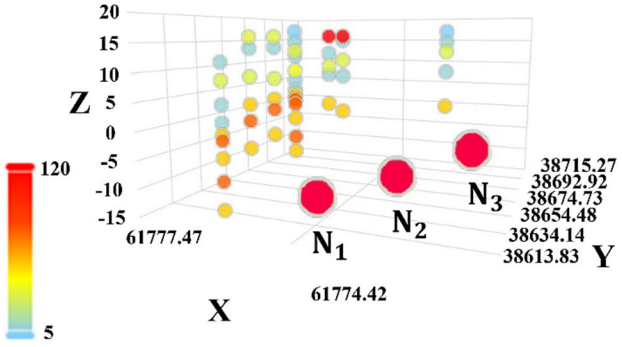

FIGURE 10. Numerical interpolation of discrete points based on mechanical properties. N_3 is the point to be assigned. N_1 and N_2 are the points already assigned.

III. RESULTS AND DISCUSSION

A. OVERVIEW OF THE ANCHOR ENGINEERING PROJECT

The anchor engineering project is located at a foundation pit slope in South China, as shown in Fig. 11. The slope excavation consists of two stages. In the first stage, the slope ratio is 1:2, and the height is 5 m, while in the second stage, the slope ratio is 1:2, and the height is 9 m. To reinforce the middle structure of the slope, 600 mixing piles are used. Additionally, there are 85 boreholes surrounding the slope.

The topography of the area varies in elevation from north to south. In the northern region, the elevation is higher, with

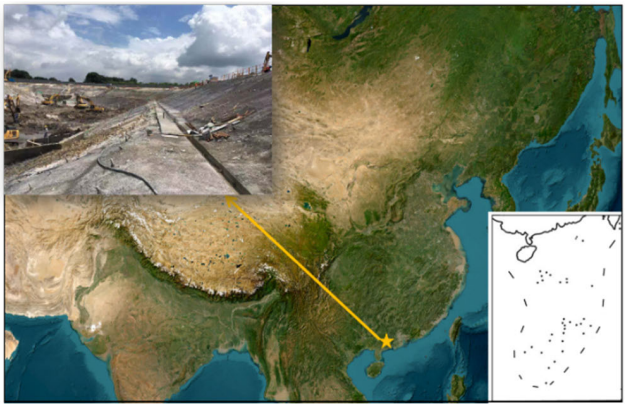

FIGURE 11. Geographic location of the engineering site. The picture in the upper left corner shows the construction site.

hills ranging from 10 m to 50 m above sea level. In contrast, the southern region consists mostly of plains with lower and flatter terrain that is less than 10 m above sea level. The specific area where this engineering project is located is characterized by hilly terrain in front of the mountains, with elevations ranging between 13 m and 22 m.

B. THREE-DIMENSIONAL INFORMATION MODEL FOR ANCHOR ENGINEERING BASED ON INCOMPLETE DATA

Data extraction involves gathering information such as borehole stratum location coordinates, stratum thickness, and stratum category from engineering geological exploration reports. These datasets are essential for conducting three-dimensional geological modeling and training an accurate neural network.

Numerical data are particularly convenient for computer recognition and calculation. The stratum categories are represented by numerical values: silt (1), fill (5), pulverized clay (10), medium coarse sand (30), slightly weathered rock (50), cave (70), medium weathered rock (90), and strongly weathered carbonaceous shale (110).

As shown in Table 1, "X", "Y", "Z", and "Stratum thickness" represent the horizontal coordinates of the plane, vertical coordinates of the plane, elevation of the center of the stratum, and thickness of the stratum, respectively. However, the available data may have missing, anomalous, or incomplete entries, which can result in the construction of inaccurate models [36]. To determine the geologic distribution, a BP neural network was used for prediction, which can also be replaced by a similar method.

According to the Fig. 4, a stratigraphic subdivision was performed to expand the dataset. The stratum data from the surrounding eight boreholes were utilized as the stratigraphy features of the central borehole, where the target value is the stratum category.

There are eight peripheral boreholes, and each borehole has an X-coordinate, a Y-coordinate, a Z-coordinate, a layer thickness, and a stratigraphic category, totaling 8*5=40 input variables. When including the positional coordinates of the center borehole and the layer thickness, there are 44 input variables. After processing the incomplete data in this manner, the amount of stratum data significantly increased, resulting in an expanded dataset with 44 samples (from 4) and thereby enhancing the accuracy of the data model.

Following the processing of the incomplete data, the 682 stratified data points were partitioned into a test set and a training set with the 10-fold cross-validation method [37], [38]. The soil category of the center borehole was used as the dependent variable, and the other data from the center borehole and the eight surrounding boreholes were used as the independent variables. These data were normalized before training was performed.

TABLE 1. Stratum data obtained from borehole loglogs. X and Y are the plane position coordinates of the borehole. Z is the stratum elevation coordinate.

Borehole number	X (m)	Y (m)	Z (m)	Stratum thickness (m)	Stratum category
Xzk4	61915.9	38593.5	17.82	1.9	5
Xzk4	61915.9	38593.5	14.07	5.6	10
Xzk4	61915.9	38593.5	9.32	3.9	30
Xzk4	61915.9	38593.5	4.82	5.1	10
…	…	…	…	…	…
Xzk4	61915.9	38593.5	−0.18	4.9	10
Xzk4	61915.9	38593.5	−2.73	0.2	50

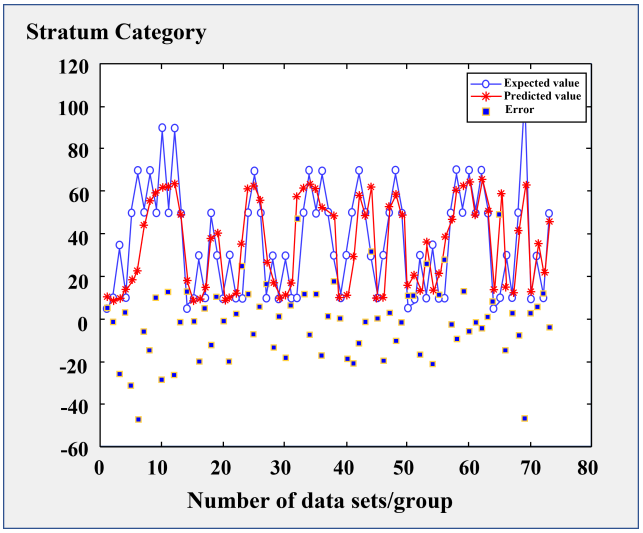

FIGURE 12. Results of neural network prediction. The two curves allow for a comparison of the actual values and predicted values.

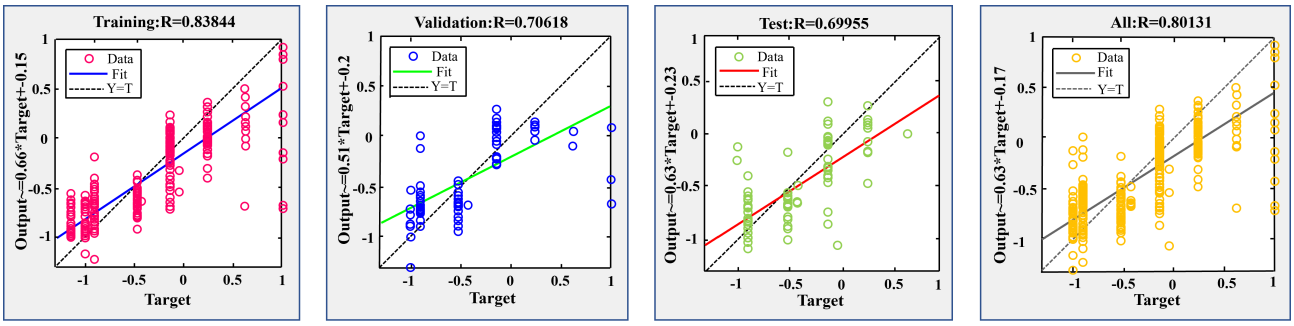

FIGURE 13. Fitting accuracy of BP neural networks with different datasets: (a) shows the results of the training dataset; (b) shows the results of the validation dataset; (c) shows the results of the test dataset; and (d) shows the results of the whole dataset.

TABLE 2. Cross-validation prediction accuracy. The ten groups of predicted results correspond to the groups in 10-fold cross-validation.

	1st group	2nd group	3rd group	4th group	5th group	6th group	7th group	8th group	9th group	10th group
Accuracy(%)	80.13	83.67	86.78	85.62	83.25	86.9	82.56	85.91	84.46	85.1

The sigmoid function was used as the activation function, the transfer function used ''purelin'', the gradient descent method was used for training, the number of training sessions was 10000, the learning efficiency was set to 0.01, and the minimum error of the training objective was set to 0.00001.

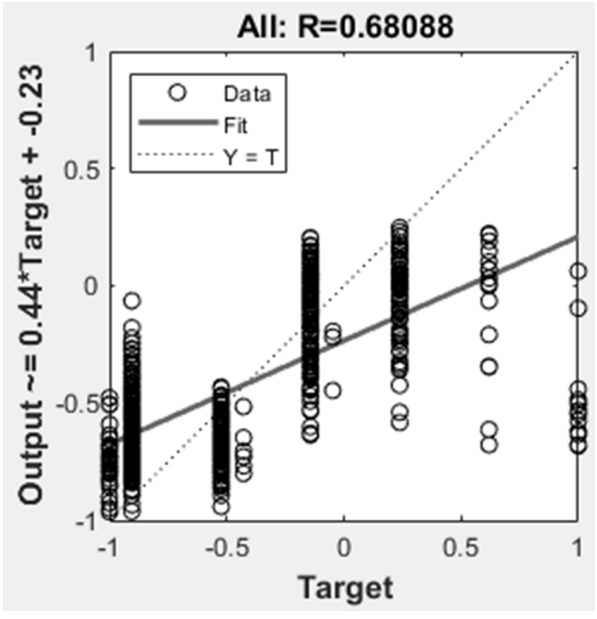

FIGURE 14. Fitting accuracy of the BP neural network based on the same dataset. The input variables excluded the surrounding boreholes.

A comparison graph was generated to illustrate the predicted values of the BP neural network and the actual values of the stratum data, as shown in Fig. 12, which demonstrates that the curve of the BP neural network prediction closely aligns with the curve of the actual stratum

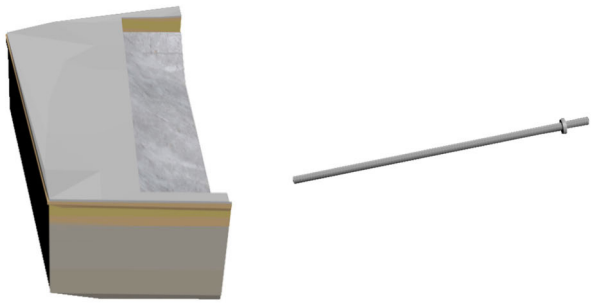

FIGURE 15. Three-dimensional model of the foundation pit slope: (a) is the geological body; (b) is the anchor component. The figure (b) is an enlarged view. The real anchors are actually smaller in size.

data. To measure the performance and accuracy of the machine learning model, three statistical indicators were introduced in the training phases: correlation coefficient (R), mean absolute error (MAE), and root mean square error (RMSE) [39], [40].

The R of the training set is 0.83844, and that of the validation set is 0.70618, indicating a better fit with less error. The MAE is 20.9994, and the RMSE is 27.1918 [41], [42]. These results suggest that the data model can achieve effective performance at this stage.

Furthermore, an accuracy graph was generated to assess the prediction accuracy of the BP neural network, as shown in Fig. 13, which shows the accuracy values of BP neural networks for different sample values, where R is the regression coefficient. The total regression coefficient of the stratum training set was found to be 0.801, indicating a strong regression performance and a higher level of accuracy for the stratum data model.

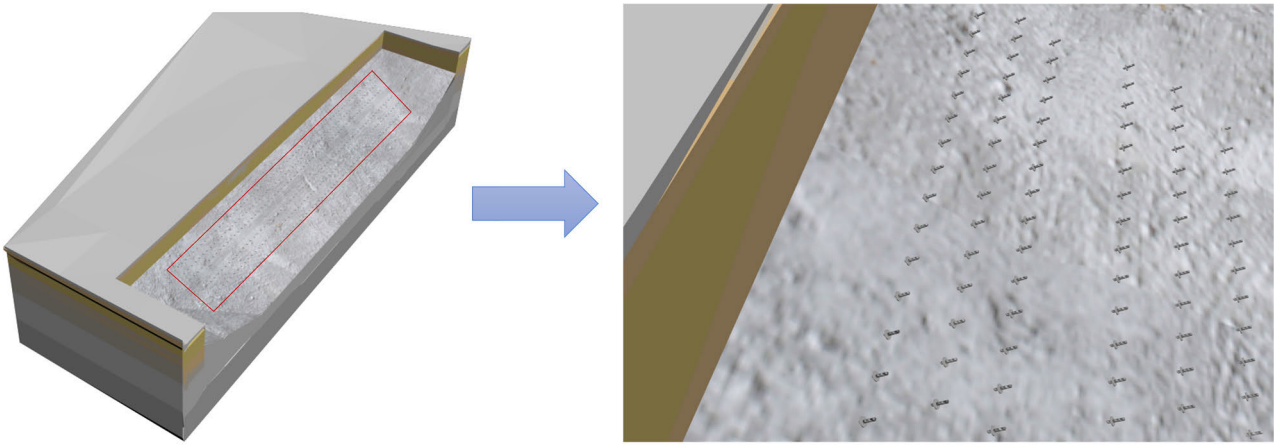

FIGURE 16. Fusion model of anchor components and the geological body: left is the overview of the whole model; right is the detailed view of anchor components.

The borehole stratum data were divided into ten groups using the 10-fold cross-validation method [43]. One group was designated as the test set, while the remaining nine groups served as the training set. The obtained scores are presented in Table 2.

After excluding the surrounding boreholes in the input variables, an R value of 0.68088 was achieved using the BP neural network, as shown in Fig. 14. The dataset used was the same as that in Fig. 13. The results showed that the method proposed in this paper improved the prediction accuracy of the neural network by 17.69% when using the whole dataset.

The geological data model generated through the prediction of BP neural network training was visualized using the three-dimensional rendering engine Three.js. During the rendering process, Three.js employs techniques such as boundary division and smoothing to enhance the visual quality of the data model. The resulting visualization provides a clear representation of the geological features for design, as depicted in Fig. 15 (a).

Based on the previous description, the geometric parameters of the anchor components underwent processing. The reference point coordinates were determined as the upper surface center of the base plate, and the range was defined accordingly. The anchor data model was subsequently rendered and visualized using Three.js. To account for the significant variations in base plate length and anchor radius, slight adjustments were made to the scale of the three-dimensional model of the anchor components. Within the context of the reference geological body, the fusion modeling of the anchor components was performed using the anchorage parameters, as shown in Fig. 15 (b). The anchors have a length of 14 m and an anchorage length of 5 m and are spaced 1 m laterally and 1.5 m vertically. The anchorage angle is set to 15°.

The starting point of the anchor was determined, and the backend server calculated the position coordinates and three-dimensional model coordinates for each anchor. These results can be utilized for the visualization of the geological body, anchor rod components, and bonding surface. To facilitate a more detailed visual observation of the anchor fusion model, the spacing and size of the anchor were adjusted accordingly, as shown in Fig. 16.

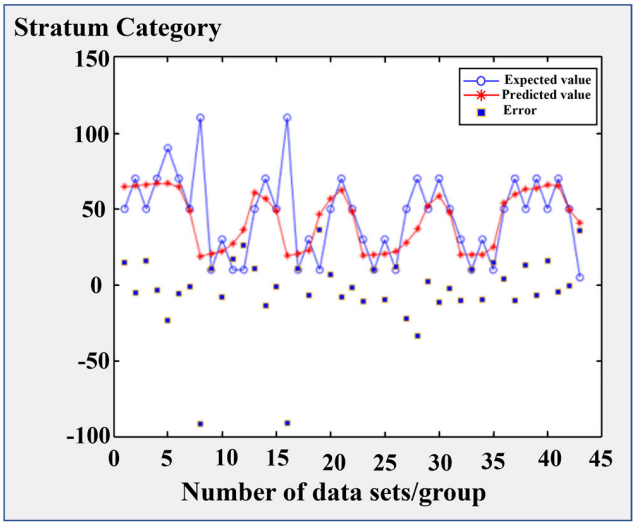

FIGURE 17. Prediction results of the neural network. The two curves show the comparison of the actual values and predicted values.

To validate the generalizability of this method, an individual model was built using another engineering project. This engineering project had a slope height of 17.8 meters, a slope coefficient of 0.202, and a total of 22 discretely distributed boreholes. Information such as the borehole location, layer thickness and layer type were extracted from the geological exploration report. These data were treated in the same way as in the former case. Later, the stratum data were divided into a dataset and a validation set and trained according to a 5-fold cross-validation method. The number of training times was 10,000, the learning efficiency was set to 0.01, and the minimum error of the training target was set to 0.00001. As shown in Fig. 17, the prediction curve and the actual stratum curve had a higher degree of fit.

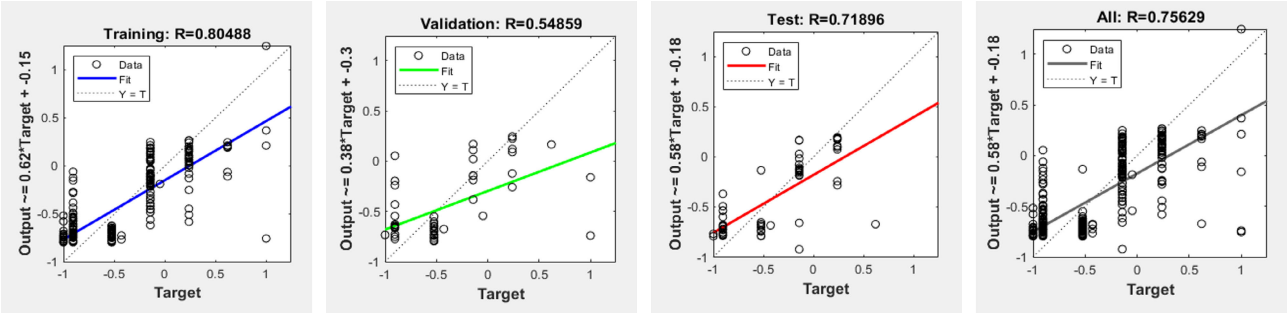

FIGURE 18. Fitting accuracy of BP neural networks with different datasets: (a) shows the results of the training dataset; (b) shows the results of the validation dataset; (c) shows the results of the test dataset; and (d) shows the results of the whole dataset.

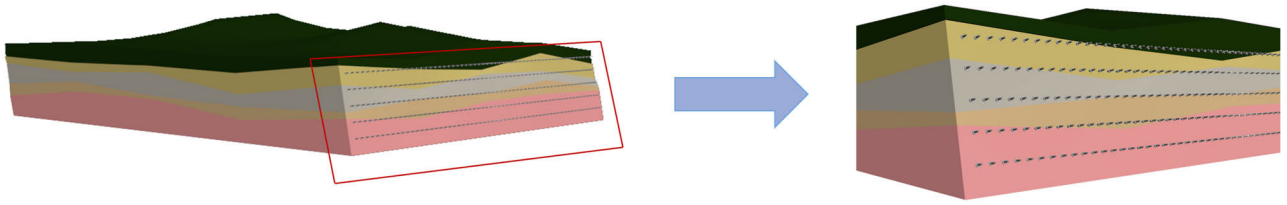

FIGURE 19. Fusion model of anchor components and the geological body: left is an overview of anchor engineering; right is a detailed view of slope. Anchor components are embedded in the geological body.

TABLE 3. Cross-validation prediction accuracy. The five groups of predicted results correspond to the groups in 5-fold cross-validation.

	1st group	2nd group	3rd group	4th group	5th group
Accuracy(%)	73.25	70.15	73.84	72.23	75.63

The MAE was 17.6407, and the RMSE was 26.7017, indicating that the algorithm effect at this time was better. From the BP neural network prediction accuracy graph, as shown in Fig. 18, it can be observed that the regression coefficient of the training set was 0.80488 and that of the test set was 0.71896. The stratum data regression performance and algorithm accuracy were good.

According to the 5-fold cross-validation method, the whole stratigraphic data were divided into five groups, the results were based on one group as the test set and the remaining four groups as the training set. The scores are shown in Table 3.

The geological body was visualized based on the dataset obtained from the BP neural network training predictions. As described earlier, the geometric parameters of the anchor members were preprocessed, with a bolt length of 14 m, an anchorage length of 5 m, an anchor spacing of 1 m in the horizontal direction, a vertical spacing of 1.5 m, and an anchor angle of 15 degrees, as shown in Fig. 19. Once the anchor starting point was determined, the background server calculated the coordinates of each anchor and the coordinates of the information model to visually model the geological body, the anchor components, and the bonding surface.

C. MULTIVARIATE INFORMATION MODEL FOR ANCHOR ENGINEERING

In the process of exploration, design, construction, and monitoring, a substantial amount of information is generated, such as mechanical properties and monitoring data. Currently, most engineering information is used only for statistical outliers. Merely collecting these data is insufficient for the optimal utilization of engineering construction. Therefore, integrating and visualizing these data with the help of the information model can effectively facilitate engineering construction [44]. By employing techniques such as machine learning, researchers can reprocess engineering data based on the information model to predict engineering hazards and perform other functions. In addition to the mentioned values of the stratigraphic category and stratigraphic coordinate, other values can be mapped. The mechanical parameters of each stratum were extracted from the exploration report and utilized to assign mechanical properties to the engineering geological body. The corresponding data are presented in Table 4. These data coupled with information models can be used in applications to industrial machine learning models. Using the borehole as a basis for grid division of the stratum, information regarding the position of each corner point can be obtained. By combining this information with the data provided in Table 4, a significant volume of discrete point mechanical property data for the geological body could be assigned.

In the first engineering, shear strength was chosen as the assignment parameter for discrete points. The visualization in Fig. 20 (a) demonstrated that certain unit spheres had been successfully assigned with mechanical data. For the

TABLE 4. Mechanical parameters of the stratum. The geological data were derived from mechanical experiments on borehole soil.

Stratum Name	Volumetric Weight $\gamma(kN/m^3)$	Angle of internal friction $\alpha(°)$	Cohesion C(kPa)	Modulus of Compressibility E_s(MPa)	Standard values for load capacity F_k(kPa)	Shear strength τ_f(MPa)	Permeability coefficient cm/s
Vegetal fill	18.5	12.0	4.0	4.0	90	/	/
Silt	16.0	4.0	5.0	2.0	40	/	10^{-7}
Medium coarse sand	19.5	26.0	0.0	/	120	/	10^{-2}
…	…	…	…	…	…	…	…
Silty clay loam	20.0	18.0	20.0	6.5	180	/	10^{-5}
Slightly weathered limestone	/	/	/	/	/	1.75	/

TABLE 5. Mechanical parameters of the anchor components.

	Underboard	Other part	Anchorage
Shear strength (MPa)	400	550	700

remaining unit spheres, interpolation was needed before rendering. Fig. 20 (b) shows the complete and continuous model.

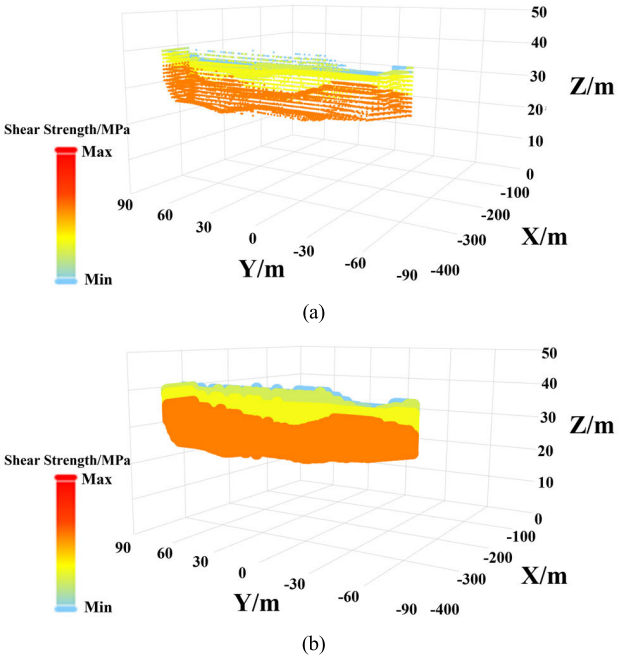

FIGURE 20. Assignment visualization schematic: (a) assignment and visualization of discrete points; and (b) color mapping after stratum interpolation.

The assignment of the mechanical properties to the anchor components involves several key steps. First, the magnitude of the mechanical parameters at each position of the anchor needs to be determined. Specifically, for this section, the shear strength of the anchor is considered as an example. Second, the assigned shear strength values are mapped to

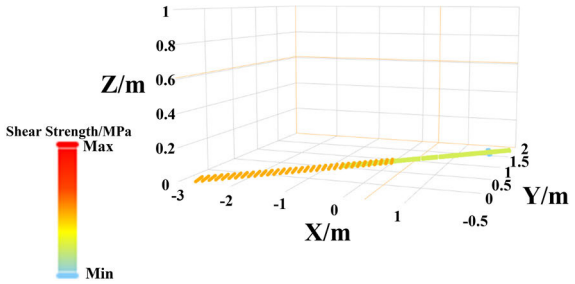

FIGURE 21. Assignment and visualization of anchor components. Different colors in the graph represent the magnitude of the shear strength properties.

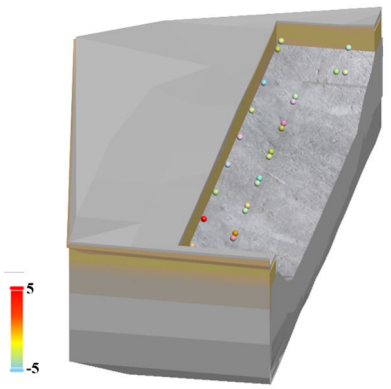

FIGURE 22. Foundation pit model with monitoring points. The different colored spheres represent different types of monitoring points.

corresponding colors for visualization purposes. Finally, the visual representation of the anchor components, including the assigned shear strength, is rendered in a client application using ECharts. The shear strength is shown in Table 5, and the effect is shown in Fig. 21.

In engineering practice, monitoring the data of the same monitoring point over different time periods is important [45]. The server records the monitoring data for each monitoring point at various intervals. For all monitoring points in anchor engineering, the visualization model can be assigned color

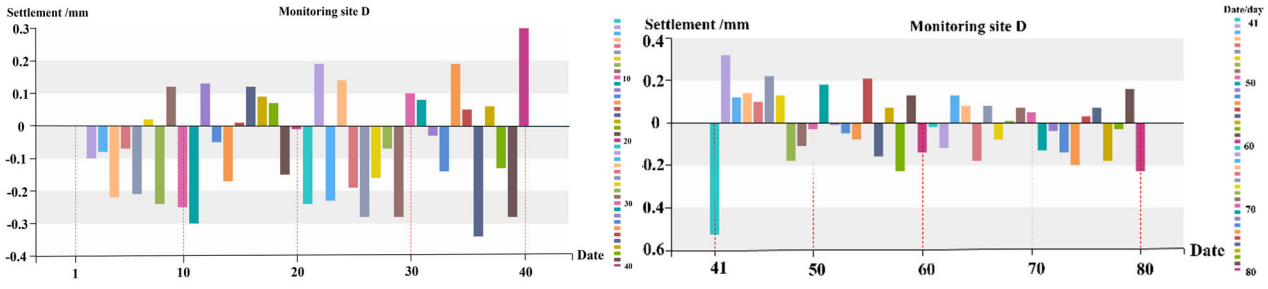

(a) (b)

FIGURE 23. Monitor point settlement changes from days 1-80: (a) settlement changes from days 1-40; (b) settlement changes from days 41-80.

TABLE 6. Comparison of modeling efficiency based on different methods. Based on the same equipment, the data isarewere obtained by designers with the same skill certificates performing the same tasks.

Modeling methods	Total work Q(m)	Working time t(h)	Modeling efficiency q(m/h)
CAD	600	13.5	44.44
Revit	600	11.3	53.10
Proposed method	600	4.5	133.33

information based on the most recent monitoring data. The locations of the monitoring points are shown in Fig. 22.

Fig. 23 illustrates a settlement data plot for different periods at monitoring point D (D represents the sensor code of the settlement monitor). Designers can observe and track the changes in the information model, which is assigned the settlement data, over time. The results show that the ground settlement was not uniform after the backfilling of the foundation pit in the karst area, and it was noteworthy that a rise and a fall occurred on the 40th and 41st days, respectively. This information is valuable for assessing the safety of engineering and making informed decisions. Historical data are stored in the server's database. By visualizing and analyzing these data, we can observe trends and identify extreme values at the monitoring points. This information is valuable for conducting an in-depth and comprehensive study of the anchor information model.

D. THREE-DIMENSIONAL INFORMATION MODEL EVALUATION

Traditional methods of model fusion in software often involve a significant amount of manual interaction and large dataset processing, which may not guarantee accuracy [46], [47]. In contrast, leveraging computer technology for integrated modeling of the geological body and anchor components can offer higher efficiency and accuracy. Three-dimensional fusion modeling using Web technology proves to be more efficient, as shown in Table 6, thus requiring less manual interaction and achieving higher accuracy compared with that of software-based fusion modeling. This approach allows for the same workload to be handled with greater efficiency and improved accuracy.

The BP neural network used for three-dimensional modeling is trained, and the evaluation of the three-dimensional model can be conducted using various metrics. In addition to the prediction accuracy, the model can be assessed by comparing the predicted values with the actual values using the BP neural network, calculating the mean square error, and visualizing information such as the gradient and generalizability transformation during the network training. The graph of predicted vs. actual values provides a visual representation of the prediction performance of the BP neural network. Additionally, other data metrics, such as the mean square error, can be utilized to assess the magnitude of the model's error, and the generalizability of the training model can be examined.

By analyzing and interpreting these data metrics, a more intuitive and concrete assessment of the three-dimensional modeling effect can be obtained, enabling adjustments to the BP neural network training model parameters to achieve an optimal model.

IV. CONCLUSION

(1) This paper proposes a method for building a three-dimensional information model, representing an intelligent design in anchor engineering. First, the original data derived from the sparse borehole are preprocessed. Second, a model of the geologic body is built by using neural network algorithms. Subsequently, anchor component modeling can be achieved according to the model parameters and design standards. Finally, the numerical engineering information is assigned to the whole three-dimensional model, which can be visualized by the render engine. This process bridges the gap between demand identification and intelligent design.

(2) The implementation is detailed and illustrated using two independent and uncorrelated engineering. The prediction accuracies of the stratum in the first case are 0.80131, improvements of up to 17.69%. This method has a shorter modeling time and higher efficiency compared with those of modeling software using the same engineering case. By mapping the engineering information to the model, the designer can gain highly valuable references for design from the information model.

(3) Other complex neural networks and rendering engines also help to enable intelligent design in anchor engineering. If there are more types of engineering information and modeling data, such as geophysical methods, the accuracy of the three-dimensional model will be higher. It is also worth mentioning that the methodology of this study requires stratum properties to have a distribution rule.

COMPETING INTERESTS STATEMENT

The authors confirm that there are no known conflicts of interest associated with this publication and there has been no significant financial support for this work that could have influenced its outcome.

DATA AVAILABILITY STATEMENT

Data is openly available in a public repository. The training and figure data used in this paper can be obtained at the following link: ''https://github.com/RockSYSU/anchor-engineering.git''.

ACKNOWLEDGMENT

(Zhang Songan and Hu Wei contributed equally to this work.)

REFERENCES

[1] D. Che and Q. Jia, ''Three-dimensional geological modeling of coal seams using weighted Kriging method and multi-source data,'' *IEEE Access*, vol. 7, pp. 118037–118045, 2019, doi: 10.1109/ACCESS.2019.2936811.

[2] Z. Liu, J. Luo, X. Wang, W. Ming, and C. Zhou, ''Unique path method of the pinch-out profile based on unified stratigraphic sequence,'' *Geosciences*, vol. 11, no. 6, p. 251, Jun. 2021, doi: 10.3390/geosciences11060251.

[3] D. D. Eneyew, M. A. M. Capretz, and G. T. Bitsuamlak, ''Toward smart-building digital twins: BIM and IoT data integration,'' *IEEE Access*, vol. 10, pp. 130487–130506, 2022, doi: 10.1109/ACCESS.2022.3229370.

[4] M. Lyu, B. Ren, B. Wu, D. Tong, S. Ge, and S. Han, ''A parametric 3D geological modeling method considering stratigraphic interface topology optimization and coding expert knowledge,'' *Eng. Geol.*, vol. 293, Nov. 2021, Art. no. 106300, doi: 10.1016/j.enggeo.2021.106300.

[5] S. Zhang, C. Peng, and C. Zou, ''An automatic method for core orientation based on planar geologic features in drill-core scans and microresistivity images,'' *IEEE Access*, vol. 10, pp. 116004–116013, 2022, doi: 10.1109/ACCESS.2022.3214197.

[6] G. Vignoli, G. Cassiani, M. Rossi, R. Deiana, J. Boaga, and P. Fabbri, ''Geophysical characterization of a small pre-alpine catchment,'' *J. Appl. Geophys.*, vol. 80, pp. 32–42, May 2012, doi: 10.1016/j.jappgeo.2012.01.007.

[7] G. Xue, H. Li, Y. He, J. Xue, and X. Wu, ''Development of the inversion method for transient electromagnetic data,'' *IEEE Access*, vol. 8, pp. 146172–146181, 2020, doi: 10.1109/ACCESS.2020.3013626.

[8] D. Jiang, Z. Zeng, S. Zhou, Y. Guan, and T. Lin, ''Integration of an aeromagnetic measurement system based on an unmanned aerial vehicle platform and its application in the exploration of the Ma'anshan magnetite deposit,'' *IEEE Access*, vol. 8, pp. 189576–189586, 2020, doi: 10.1109/access.2020.3031395.

[9] B. K. Yahşi and H. Ersoy, ''Effect of mineralogical composition related to profile depth on index and strength properties of regolith soil,'' *Bull. Eng. Geol. Environ.*, vol. 80, no. 2, pp. 1791–1808, Feb. 2021, doi: 10.1007/s10064-020-01968-8.

[10] B. Schaaf, C. Richter, M. Feldmann, E. Toups, J. Simon, S. Reese, R. Seewald, A. Schiebahn, and U. Reisgen, ''Material parameter determination for the simulation of hyperelastic bonds in civil engineering considering a novel material model,'' *Int. J. Adhes. Adhesives*, vol. 103, Dec. 2020, Art. no. 102692, doi: 10.1016/j.ijadhadh.2020.102692.

[11] F. Li, A. Jiang, and S. Zheng, ''Anchoring parameters optimization of tunnel surrounding rock based on particle swarm optimization,'' *Geotech. Geolog. Eng.*, vol. 39, no. 6, pp. 4533–4543, Aug. 2021, doi: 10.1007/s10706-021-01782-3.

[12] M. Rossi, R. Wisén, G. Vignoli, and M. Coni, ''Assessment of distributed acoustic sensing (DAS) performance for geotechnical applications,'' *Eng. Geol.*, vol. 306, Sep. 2022, Art. no. 106729, doi: 10.1016/j.enggeo.2022.106729.

[13] J. Ouyang, C. Zhou, Z. Liu, and G. Zhang, ''Triangulated irregular network-based probabilistic 3D geological modelling using Markov chain and Monte Carlo simulation,'' *Eng. Geol.*, vol. 320, Jul. 2023, Art. no. 107131, doi: 10.1016/j.enggeo.2023.107131.

[14] C. Zhuang, H. Zhu, W. Wang, B. Liu, Y. Ma, J. Guo, C. Liu, H. Zhang, F. Liu, and L. Cui, ''Research on urban 3D geological modeling based on multi-modal data fusion: A case study in Jinan, China,'' *Earth Sci. Informat.*, vol. 16, no. 1, pp. 549–563, Nov. 2022, doi: 10.1007/s12145-022-00897-2.

[15] Q. Jia, W. Li, and D. Che, ''A triangulated irregular network constrained ordinary Kriging method for three-dimensional modeling of faulted geological surfaces,'' *IEEE Access*, vol. 8, pp. 85179–85189, 2020, doi: 10.1109/ACCESS.2020.2993050.

[16] Q. Zeng, W. Ming, Z. Zhang, Z. Du, Z. Liu, and C. Zhou, ''Construction of a 3D stratum model based on a solid model,'' *IEEE Access*, vol. 9, pp. 20760–20767, 2021, doi: 10.1109/ACCESS.2021.3053628.

[17] Z. Zhang, Z. Yin, and X. Yan, ''A workflow for building surface-based reservoir models using NURBS curves, coons patches, unstructured tetrahedral meshes and open-source libraries,'' *Comput. Geosci.*, vol. 121, pp. 12–22, Dec. 2018, doi: 10.1016/j.cageo.2018.09.001.

[18] X. Zhang, C. Chen, Z. Xu, and H. Li, ''Method and application of urban 3D rapid modeling of geology based on CAD borehole logs,'' *Geofluids*, vol. 2022, pp. 1–12, May 2022, doi: 10.1155/2022/4959887.

[19] H. Si-Jie, G. Yu-Bin, Y. Chang-Yi, W. Xiao, and W. Qi-Zhi, ''Research on modeling method of 3D geological entity model based on BIM,'' in *Proc. E3S Web Conf.*, vol. 198, 2020, Art. no. 02031, doi: 10.1051/e3sconf/202019802031.

[20] R. Song, X. Qin, Y. Tao, X. Wang, B. Yin, Y. Wang, and W. Li, ''A semi-automatic method for 3D modeling and visualizing complex geological bodies,'' *Bull. Eng. Geol. Environ.*, vol. 78, no. 3, pp. 1371–1383, Apr. 2019, doi: 10.1007/s10064-018-1244-3.

[21] L. Jones and P. Hobbs, ''The application of terrestrial LiDAR for geohazard mapping, monitoring and modelling in the British geological survey,'' *Remote Sens.*, vol. 13, no. 3, p. 395, Jan. 2021, doi: 10.3390/rs13030395.

[22] T. Nemoto, S. Masumoto, V. Raghavan, S. Nonogaki, and F. Nakada, ''Development of open source web-GIS platform for three-dimensional geologic modeling and visualization,'' *Spatial Inf. Res.*, vol. 28, no. 6, pp. 645–653, Dec. 2020, doi: 10.1007/s41324-020-00321-1.

[23] X. He, T. O. Sonnenborg, F. Jørgensen, and K. H. Jensen, ''Modelling a real-world buried valley system with vertical non-stationarity using multiple-point statistics,'' *Hydrogeol. J.*, vol. 25, no. 2, pp. 359–370, Mar. 2017, doi: 10.1007/s10040-016-1486-8.

[24] J. Zhao, M. Shi, G. Hu, X. Song, C. Zhang, D. Tao, and W. Wu, ''A data-driven framework for tunnel geological-type prediction based on TBM operating data,'' *IEEE Access*, vol. 7, pp. 66703–66713, 2019, doi: 10.1109/ACCESS.2019.2917756.

[25] Y. Liu, C. Shi, Q. Wu, R. Zhang, and Z. Zhou, ''Visual analytics of stratigraphic correlation for multi-attribute well-logging data exploration,'' *IEEE Access*, vol. 7, pp. 98122–98135, 2019, doi: 10.1109/ACCESS.2019.2929061.

[26] J. Guo, Z. Wang, C. Li, F. Li, M. W. Jessell, L. Wu, and J. Wang, ''Multiple-point geostatistics-based three-dimensional automatic geological modeling and uncertainty analysis for borehole data,'' *Natural Resour. Res.*, vol. 31, no. 5, pp. 2347–2367, Oct. 2022, doi: 10.1007/s11053-022-10071-6.

[27] C. Xia, Z. Liu, C. Zhou, and L. Zhang, "A meso/macroscale theoretical model for investigating the large deformation of soft rock tunnels considering creep and anisotropic effects," *Rock Mech. Rock Eng.*, vol. 56, no. 7, pp. 4901–4922, Jul. 2023, doi: 10.1007/s00603-023-03306-2.

[28] J. Hamidzadeh and M. Moradi, "Enhancing data analysis: Uncertainty-resistance method for handling incomplete data," *Int. J. Speech Technol.*, vol. 50, no. 1, pp. 74–86, Jan. 2020, doi: 10.1007/s10489-019-01514-4.

[29] J. Ching and K.-K. Phoon, "Constructing a site-specific multivariate probability distribution using sparse, incomplete, and spatially variable (MUSIC-X) data," *J. Eng. Mech.*, vol. 146, no. 7, Jul. 2020, Art. no. 04020061, doi: 10.1061/(ASCE)EM.1943-7889.0001779.

[30] C. Bai, J. Guo, and H. Zheng, "Three dimensional vibration-based terrain classification for mobile robots," *IEEE Access*, vol. 7, pp. 63485–63492, 2019, doi: 10.1109/ACCESS.2019.2916480.

[31] E. Collini, L. A. I. Palesi, P. Nesi, G. Pantaleo, N. Nocentini, and A. Rosi, "Predicting and understanding landslide events with explainable AI," *IEEE Access*, vol. 10, pp. 31175–31189, 2022, doi: 10.1109/access.2022.3158328.

[32] H. M. Shakeel, S. Iram, H. Al-Aqrabi, T. Alsboui, and R. Hill, "A comprehensive state-of-the-art survey on data visualization tools: Research developments, challenges and future domain specific visualization framework," *IEEE Access*, vol. 10, pp. 96581–96601, 2022, doi: 10.1109/ACCESS.2022.3205115.

[33] M. F. Kucuk and I. Uysal, "Anomaly detection in self-organizing networks: Conventional versus contemporary machine learning," *IEEE Access*, vol. 10, pp. 61744–61752, 2022, doi: 10.1109/ACCESS.2022.3182014.

[34] K. Mei, X. Li, X. Zhang, Y. Sun, Y. Li, and S. Sun, "Short-term performance of new composite anchorage with multiple CFRP tendons," *J. Compos. Constr.*, vol. 27, no. 2, Apr. 2023, Art. no. 04023016, doi: 10.1061/JCCOF2.CCENG-4068.

[35] L. Consalvi, W. Didimo, G. Liotta, and F. Montecchiani, "BrowVis: Visualizing large graphs in the browser," *IEEE Access*, vol. 10, pp. 115776–115786, 2022, doi: 10.1109/ACCESS.2022.3218884.

[36] S. Yu, T. Chen, and G. Hu, "Confidence-constrained support vector regression for geological surface uncertainty modeling," *IEEE Access*, vol. 8, pp. 182451–182461, 2020, doi: 10.1109/ACCESS.2020.3028932.

[37] J. Khatti and K. S. Grover, "Prediction of compaction parameters for fine-grained soil: Critical comparison of the deep learning and standalone models," *J. Rock Mech. Geotech. Eng.*, vol. 15, no. 11, pp. 3010–3038, Nov. 2023, doi: 10.1016/j.jrmge.2022.12.034.

[38] J. Khatti and K. S. Grover, "CBR prediction of pavement materials in unsoaked condition using LSSVM, LSTM-RNN, and ANN approaches," *Int. J. Pavement Res. Technol.*, to be published, doi: 10.1007/s42947-022-00268-6.

[39] J. Khatti and K. S. Grover, "Prediction of compaction parameters of compacted soil using LSSVM, LSTM, LSBoostRF, and ANN," *Innov. Infrastruct. Solutions*, vol. 8, no. 2, p. 76, Jan. 2023, doi: 10.1007/s41062-023-01048-2.

[40] J. Khatti and K. S. Grover, "Prediction of UCS of fine-grained soil based on machine learning—Part 2: Comparison between hybrid relevance vector machine and Gaussian process regression," *Multiscale Multidisciplinary Model., Exp. Des.*, to be published, doi: 10.1007/s41939-023-00191-8.

[41] T. Pradeep, A. Bardhan, A. Burman, and P. Samui, "Rock strain prediction using deep neural network and hybrid models of ANFIS and meta-heuristic optimization algorithms," *Infrastructures*, vol. 6, no. 9, p. 129, Sep. 2021, doi: 10.3390/infrastructures6090129.

[42] N. Chakraborty, C. F. Lui, and A. Maged, "A distribution-free change-point monitoring scheme in high-dimensional settings with application to industrial image surveillance," *Commun. Statist. Simul. Comput.*, pp. 1–17, Apr. 2023, doi: 10.1080/03610918.2023.2202371.

[43] C. Qi, J. Diao, and L. Qiu, "On estimating model in feature selection with cross-validation," *IEEE Access*, vol. 7, pp. 33454–33463, 2019, doi: 10.1109/ACCESS.2019.2892062.

[44] M. Zhou, H. Liu, and Z. Wang, "Can smart city construction promote the level of public services? Quantitative evidence from China," *IEEE Access*, vol. 10, pp. 120923–120935, 2022, doi: 10.1109/ACCESS.2022.3221759.

[45] C. Zhu, Z. Yan, Y. Lin, F. Xiong, and Z. Tao, "Design and application of a monitoring system for a deep railway foundation pit project," *IEEE Access*, vol. 7, pp. 107591–107601, 2019, doi: 10.1109/ACCESS.2019.2932113.

[46] L. Li and C. Mao, "Big data supported PSS evaluation decision in service-oriented manufacturing," *IEEE Access*, vol. 8, pp. 154663–154670, 2020, doi: 10.1109/ACCESS.2020.3018667.

[47] R. Roscher, B. Bohn, M. F. Duarte, and J. Garcke, "Explainable machine learning for scientific insights and discoveries," *IEEE Access*, vol. 8, pp. 42200–42216, 2020, doi: 10.1109/ACCESS.2020.2976199.

ZHANG SONGAN is currently pursuing the master's degree with the School of Civil Engineering, Sun Yat-sen University. His research interests include rock engineering, engineering intelligent control, and engineering informationization.

HU WEI is currently pursuing the Ph.D. degree with the School of Civil Engineering, Sun Yat-sen University. His research interests include rock and soil mechanics, and information model technology.

ZENG LIANG is currently pursuing the master's degree with the School of Civil Engineering, Sun Yat-sen University. His research interests include slope engineering, landslide stability, and three dimensional modeling.

YANG JUNJIE is currently pursuing the master's degree with the School of Civil Engineering, Sun Yat-sen University. His research interests include foundation pit engineering and model visualization.

ZHONG YUSEN is currently pursuing the master's degree with the School of Civil Engineering, Sun Yat-sen University. His research interest includes intelligent model development.

LIU ZHEN is currently an Associate Professor with the School of Civil Engineering, Sun Yat-sen University. He has been the Principal Investigator of more than 20 national and provincial research projects, including the Special Project of National Key Research and Development Plan, the National Natural Science Foundation of China (General Program), the Youth Fund Project, the Ph.D. Programs Foundation of the Ministry of Education of China, the Special Key Project of Application in Guangdong, and the Guangdong Natural Science Foundation Project. He has published more than 50 peer-reviewed and conference papers. His research interests include catastrophic mechanism of geomaterials, such as soft rock and expansive soil, and experimental equipment design and development of monitoring and warning technology. He also serves as the Executive Director for the Soft Rock Engineering and Deep Disaster Control Branch, Chinese Society for Rock Mechanics and Engineering, the Director for the Institute of Geotechnical Mechanics and Engineering of Guangdong, and the Vice Chairperson for the Youth Committee.

ZHOU CUIYING received the M.Sc. and Ph.D. degrees from the China University of Geosciences. She is currently the Leader of the Grand Research Team of Geotechnical Engineering, School of Civil Engineering, Sun Yat-sen University. She has been the PI of more than 50 national and provincial research projects, including the National Natural Science Foundation of China (Key Program), the National Natural Science Foundation of China (Instrument Orientated), the National 863 Project, and the Scientific and Technology Advancement Project jointly supported by the Ministry of Education and Guangdong Province. She has published 260 journal articles (including 130 SCI/EI papers). With a focus on the safety issue of practical engineering projects, her research interests include catastrophic mechanism and early-warning method of geotechnical disasters in soft rock and soft soil area, new generation test equipment, monitoring and warning technology, intelligent platform for early-warning and disaster prevention, new materials, technologies and standards for ecological restoration and protection. She is a member of the International Society for Rock Mechanics and Engineering and the International Society for Engineering Geology and the Environment.